Energy performance of diaphragm walls used as heat exchangers

Alice Di Donna Politecnico di Torino, Department of Structural, Building and Geotechnical Engineering, Torino, Italy

Francesco Cecinato University of Trento, Department of Civil, Environmental and Mechanical Engineering, Trento, Italy

Fleur Loveridge*University of Leeds, School of Civil Engineering, UK (formally University of Southampton, UK)

Marco Barla Politecnico di Torino, Department of Structural, Building and Geotechnical Engineering, Torino, Italy

* corresponding author – F.A.Loveridge@leeds.ac.uk; University of Leeds, School of Civil Engineering, Woodhouse Lane, Leeds, UK; 0044 (0)7773346203

Date of revision: 22nd September 2016

Number of words in revised main text: 5119

12 Tables and 7 Figures

Energy performance of diaphragm walls used as heat exchangers

Abstract

The possibility of equipping diaphragm walls as ground heat exchangers to meet the full or partial heating and cooling demands of overlying or adjacent buildings has been explored in recent years. In this paper, the factors affecting the energy performance of diaphragm walls equipped as heat exchangers are investigated through finite element modelling. The numerical approach employed is first validated using available experimental data and then applied to perform parametric analyses. Parameters considered in the analysis include panel width, the ratio between the wall and excavation depths, heat transfer pipe spacing, concrete cover, heat-carrier fluid velocity, concrete thermal properties and the temperature difference between the air within the excavation and the soil behind the wall. The results indicate that increasing the number of pipes by reducing their spacing is the primary route to increasing energy efficiency in the short term. However, the thermal properties of the wall concrete and the temperature excess within the excavation space are also important, with the latter becoming the most significant in the medium to long term. This confirms the benefits of exploiting the retaining walls installed for railway tunnels and metro stations where additional sources of heat are available.

Keywords

Diaphragm walls & in situ test

Thermal effects

Renewable energy

Energy performance of diaphragm walls used as heat exchangers

1. Introduction

Energy geostructures are an interesting and promising technology to tackle the increasing energy demand for heating and cooling of buildings and other infrastructure, through use of a local and sustainable source. However, a correct and optimised design is of fundamental importance to deliver an energy efficient solution.

Several authors have already studied the efficiency of energy geostructures. However, this has mainly concerned energy piles, for example see Cecinato & Loveridge (2015); Loveridge & Cecinato (2016); Batini et al. (2015). Parametric analyses performed to investigate the relative influence of different parameters on the heat exchange potential of energy geostructures have also been carried out by the authors. In particular, Cecinato and Loveridge (2015) studied the influence of a number of engineering parameters on the energy efficiency of thermoactive piles, while Di Donna & Barla (2015) studied the influence of underground conditions on the heat exchange capacity of energy tunnels. Both these aspects are essential to define the efficiency of energy geostructures in each specific case.

Despite the increasing interest for such applications, relative little work has been carried out on the study of diaphragm walls converted to energy geostructures (Bourne-Webb et al. 2016; Bourne-Webb et al. 2015; ICConsulten 2005; Sterpi et al. 2014; Di Donna 2016). Certainly, there has been no rigorous parametric assessment of the capability of energy diaphragm walls, and few attempts to fully justify design choices and assumptions.

The aim of this paper is to apply statistically based parametric analysis techniques to the energy assessment of diaphragm walls, and draw conclusions related to the optimisation of their energy efficiency. To do this a numerical technique has been employed in conjunction with a statistical analysis, to limit the number of simulations required and rationally interpret the results. Before outlining the statistical analysis and the numerical approach adopted, this paper first reviews constructed energy diaphragm wall case studies and previous relevant analyses to permit appropriate design of the numerical study.

2. Past Experience of Energy Diaphragm Walls

Records of constructed energy diaphragm walls are available from the UK, Austria and China (Table 1). In addition, some studies that provide details of the energy that may be available from the inside spaces of underground infrastructure, e.g. tunnels, metro stations are shown in Table 2 and Table 3. Using this data and typical construction conditions for diaphragm walls more generally, sections 2.1 and 2.2 review the appropriate geometry and boundary conditions to be used in the numerical and statistical studies.

2.1. Geometry

Diaphragm walls are often used for the support of deep excavations where other techniques may be unsuitable. These include cases at greater depths and where cut off functions are important. A large number of case studies are presented by Gaba et al. (2003), as well as general indications of typical practice by Burland et al. (2012). These suggest that walls are typically 0.8 m to 1.2 m in width (W in Figure 1), with depths typically between 10 m and 40 m (D in Figure 1). Previous work (Cecinato & Loveridge 2015) suggests that the length of the wall will be of great influence in the energy efficiency of the geostructure. However, with diaphragm walls there is the additional consideration of how much of the wall is embedded within the soil and how much is open on one side to the excavation (H in Figure 1). These two parts of the wall would be expected to experience

different rates of heat transfer due to the differing boundary conditions. Other geometric factors that may affect the energy exchanged include the number (and/or spacing, sp in Figure 1) of installed heat transfer pipes, whether these are fixed to both sides of the walls and what distance they are from the wall edge (the concrete cover, C in Figure 1). Where possible, constructed values for these parameters have been extracted from the literature and are summarised in Table 1. It can be seen that typical Austrian construction includes pipes on both sides of the walls. However, the pipes on the excavation side are only included in the embedment section of the wall. This has been possible in these cases as the steel cage to which the pipes are fixed is constructed in one piece. This means that pipes can all be placed on the steel in advance. This type of construction is not possible where constraints mean that the cage must be spliced on site. In such cases, the pipes are typically placed only on the soil side of the wall and are restricted to vertical arrangements.

2.2. Boundary conditions

A key difference between diaphragm walls and more traditional types of ground heat exchanger is their exposure to the air on one side for some proportion of their depth. The space within the excavation that the wall supports may be used for a number of different functions, the most common being basements, underground car parks, metro stations or shallow light rail tunnels. Those applications where there is potentially a source of heat, e.g. rail tunnels and metro stations, may be more suitable for efficient heat extraction, but potentially less suitable for applications in heat disposal.

There are few case studies in the literature, for which a thorough assessment of the internal boundary condition for energy diaphragm walls is made. Those where analysis of energy exchange has been carried out, either use a constant temperature boundary or assume a convective heat flux (q, W/m^2) determined by a heat transfer coefficient (h, W/m^{2}K) and the temperature difference between the wall, T_{wall}, and the space, T_{exc}:

$$q = h(T_{exc} - T_{wall}) \quad \textbf{(1)}$$

Bourne Webb et al. (2016) investigated the effect of applying the two different types of boundary condition. For the long term they concluded that imposing constant temperature could be non-conservative with respect to heating capacity, although if airflow in the excavation is faster than 3 to 5 m/s (as it might occur for instance in tunnels), this assumption will not be too far in error. Studies that considered a constant temperature boundary condition include Kurten et al. (2015), Kurten (2014), Rui (2014), Soga et al. (2014) and Sterpi et al. (2014) who all conducted numerical analysis. Kurten considered basement applications, whereas Rui and Soga et al were considering metro stations. The analysis of Sterpi et al. is more generic. None of the above authors provides a comprehensive rationale for use of this type of boundary condition, although Kurten was validating large-scale laboratory experiments so there is some justification for the considered approach.

Studies where a heat-transfer coefficient approach is adopted are summarised in Table 2. Some justification for this approach can be found in ISO 6946 (BS EN ISO 6946:2007 2007) where surface heat transfer coefficients are quoted for internal and external spaces in the built environment. Depending on the direction of heat flow and the case, general values between 6 W/m^{2}K and 20 W/m^{2}K are suggested. ISO 6949 also provides guidance on linking wind speeds to heat transfer coefficients, suggesting that values in excess of 50 W/m^{2}K could be achieved with speeds of 10 m/s. However, caution should be applied when using such high values. While Ampofo et al. (2004) suggest that wind speeds of 10 m/s could be achieved in the London underground system, heat transfer estimates from the current Crossrail constructions suggest that much lower values would be achieved in reality (Nicholson et al. 2014). Data related to the tunnel internal temperature are also available in the literature and summarised in Table 3. These vary seasonally, generally in response to the external air temperature, and are usually higher than the original undisturbed ground temperature.

3. Parametric analysis design

3.1. Choice of parameters

The choice of the design parameters to be investigated and their range of variability was based on the literature review presented above and the experience gained from existing engineering projects and previous works carried out by the authors and other researchers on energy geostructures. From previous studies on energy piles (Cecinato & Loveridge 2015), it appeared that the wall length would be one of the most important parameters affecting energy performance. This was therefore taken as an implicit assumption of the study and instead the ratio R between the panel height D and the excavation depth H was chosen for investigation, together with the panel width W (Figure 1). The former was expected to be significant since it controls the proportion of the wall area exchanging heat with the excavation.

Two other important parameters, which will be considered in the parametric analysis, are the velocity of the heat carrier fluid, hereafter referred to as v, and the number of pipes. Here the latter is characterised by the pipes spacing, sp. Previous analyses showed that the pipes diameter does not significantly affect the energy efficiency, thus it was not considered in the parametric analysis (Cecinato & Loveridge 2015; Loveridge & Cecinato 2016). Also the panel length, L, being quite standard in geotechnical projects and unlikely to be engineered based on thermal considerations, was kept fixed in all the numerical simulations. The thermal properties of the materials clearly play an important role. However, assuming that the heat transfer in the ground is mainly governed by conduction while ground water flow is negligible, the parameters that will be most influential are the thermal conductivity and diffusivity of concrete and soil and the undisturbed ground temperature (Cecinato & Loveridge 2015; Di Donna & Barla 2015). Given that the properties of the ground cannot be engineered at a given site, the study focused on the influence of the concrete thermal conductivity, hereafter referred to as λ_{con}. Considering that also the air temperature inside the excavation is expected to influence the results significantly for diaphragm walls, the difference between the soil and excavation air temperature, ΔT, was also included in the parametric analysis.

For the sake of simplicity, and based on the conclusions outlined by Bourne Webb et al. (2016) and Bourne-Webb et al. (2015), a constant temperature boundary condition was imposed on the excavation side, neglecting the heat transfer convective component. In the long term this assumption is more representative of tunnels, and other applications where high airflow persists (Bourne-Webb et al. 2016). However, in contrast to Bourne Webb et al. (2016), which applied steady state thermal analysis, this study will be transient and consider the changing impact of the different parameters with time. The full list of parameters considered in this study and their range of variability are summarised in Table 4.

3.2. Statistical method

Reference was made to the concepts of Engineering Statistics, in particular to the so-called Experimental design method, that deals with deliberately changing one or more variables in a process, to observe the effect that the changes have on a response variable. Among the available experimental design techniques, the Taguchi method was selected for its robustness, simplicity and adaptability to engineering problems (Taguchi et al. 1989; Peace 1993; Cecinato & Zervos 2012; Cecinato 2009; Cecinato et al. 2015). A fundamental step in Taguchi analysis is the definition of a suitable 'orthogonal array', i.e., a 2-dimensional matrix defining the variable settings for each of the experiments (i.e., numerical simulations in this case) needed. Table 5a shows the Taguchi orthogonal array used in this case. Each row of the matrix contains the list of settings for all parameters in one experiment. Each column of the array corresponds to one of the variables, and contains all the values that this variable will be assigned during the numerical experiments. Hence the values in the columns for each row refer to the level of the parameters used in each experiment. Since only two levels are contained in Table 5a (level 1 and level 2), these represent the lower and upper bounds of the chosen parameters given in Table 4.

The essential property of the orthogonal array is 'statistical independence'. Within each column an equal number of occurrences for each level is present. For example, in

a, in each column both level 1 and level 2 occur four times. Additionally, the columns are mutually orthogonal, i.e. for each level within one column, each level within any other column will occur an equal number of times. For example, in the first column of Table 5a, level 1 occurs in the first four rows, in correspondence of which levels 1 and 2 occur twice in all other columns. A given parameter has a strong impact on the output variable if the results associated with one of its levels are very different from the results associated with another one of its levels. Since, due to orthogonality, the levels of all other parameters occur an equal number of times for each level of this given parameter, their effect will be cancelled out in the computation of the given parameter's effect. The estimation of the effect of any one particular parameter will then tend to be accurate and reproducible (Peace 1993).

With the above settings, a Taguchi analysis will need only eight simulations (experiments) to be completed, followed by some basic statistical analysis of the results (so-called level average analysis, see section 5.1). In contrast, with the "full factorial" method (i.e., running a simulation for each one of the possible combinations of parameters) the number of simulations needed would be 7^2=49. The advantage of adopting the Taguchi method is thus apparent, as it allows substantial time saving whilst ensuring the significance of results. In fact, not only does the fundamental property of statistical independence warrant representativeness of results, but it is also possible to double-check the reliability of the analysis by performing confirmation runs (refer to section 5.1 and Peace 1993; Cecinato 2009; Cecinato & Zervos 2012).

An "L8" seven parameters set with two levels each was chosen to be the most suitable for the considered situation. The corresponding "L8" orthogonal array is readily available in the literature (e.g. Peace 1993) and reported in Table 5a. In the array, the seven parameters to be investigated correspond to the seven columns, while the eight simulations required are reported in the eight rows. For each parameter, the two levels (lower- and upper-bound values) are referred to as 1 and 2, respectively. The array can thus be filled in with the parameters' settings from Table 4 to finalise the parametric study design, leading to the array presented in Table 5b.

4. Numerical approach

To perform the eight runs defined in Table 5b and simulate the thermal exchange between the fluid circulating in the pipes, the concrete wall and the surrounding saturated soil, numerical modelling was carried out by means of the finite element software FEFLOW© (Diersch 2009). The convection-diffusion problem is governed by the following equations, written in the Eulerian coordinate system for a saturated medium composed by a solid and a liquid (water) phase:

- Mass conservation equation:

$$S \cdot \partial_t p + \nabla \cdot \left(n v_{w,i}\right) = 0 \quad \textbf{(2)}$$

where ∂_t and $\nabla \cdot$ denote the time derivative and the divergence operator , $S = [n\Upsilon_w + (1-n)\Upsilon_s]$ is the specific storage coefficient, n the porosity, Υ_w and Υ_s the water and solid compressibility, p the pressure and $v_{w,i}$ the vector of water velocity with respect to the solid skeleton.

- The Darcy's fluid velocity ($v_{f,i}$) law:

$$v_{f,i} = n v_{w,i} = -\frac{k_{ij}\rho_w g_i}{\mu}\nabla h = -K_{ij}\nabla h \quad \textbf{(3)}$$

where k_{ij} is the intrinsic hydraulic conductivity tensor (expressed in m^2), ρ_w the water density, g_i the gravity vector, μ the water dynamic viscosity, K_{ij} the hydraulic conductivity (expressed in m/s) and h the hydraulic head defined as:

$$h = \frac{p}{\rho_w g_i} + y \tag{4}$$

where y is the vertical coordinate.

- The energy conservation equation:

$$[n\rho_w c_w + (1-n)\rho_s c_s]\partial_t T + n\rho_w c_w v_{w,i}\nabla \mathrm{T} - \nabla \cdot \left(\lambda_{ij}\nabla \mathrm{T}\right) = 0 \tag{5}$$

where ∇ denotes the gradient operator, c_w and c_s are the water and solid phase heat capacities, ρ_s is the solid phase density and T is the temperature. The term λ_{ij} includes the heat conduction and the dispersion components, as:

$$\lambda_{ij} = [n\lambda_w + (1-n)\lambda_s]\delta_{ij} + \rho_w c_w \left[\alpha_T \sqrt{v_{w,i} v_{w,j}}\delta_{ij} + (\alpha_L - \alpha_T)\frac{v_{w,i} v_{w,j}}{\sqrt{v_{w,i} v_{w,j}}}\right] \tag{6}$$

where λ_w and λ_s are the water and solid phase thermal conductivities, δ_{ij} the Kronecker delta, α_T and α_L the longitudinal and transverse thermal dispersivity.

In the analyses presented, the absorber pipes were reproduced by special 1D elements built into the software FEFLOW©. In these elements the thermal resistance of the plastic pipes is neglected. This could lead to a very small temperature error in the calculations presented. However, the use of the 1D pipe elements has been validated for similar systems and showed good agreement when compared to analytical solutions (Diersch 2009). Additional energy wall specific validation is included below.

It should be also remarked that despite the above model being capable of dealing with flowing groundwater conditions, in this work the convective component of heat exchange due to flowing groundwater has been neglected for simplicity.

4.1. Numerical model validation

The numerical approach was first validated against experimental data provided by Xia et al. (2012) and Sun et al. (2013). A 38 m depth energy diaphragm wall with a 18.5 m excavation was tested in situ by circulating fluid through heat transfer pipes embedded in the wall. The wall panel was 2.25 m wide and 1.0 m thick. A single U-pipe arrangement was used with a spacing of 75 cm between the pipes and a concrete cover of 10 cm (Figure 2a). The geometry of the numerical model is illustrated in Figure 2b. The pipes had an external diameter of 25 mm and thickness of 2.3 mm. The heat carrier fluid velocity was set equal to 0.6 m/s, its inlet temperature was kept constant to 35 °C for a test duration of 2 days. The soil temperature was initially measured equal to 16.3 °C, the external air temperature equal to 10.6 °C and the wall temperature equal to 23 °C. Accordingly, constant external air temperature was applied on the top boundary, excavation plane and wall side towards the excavation, while constant soil temperature was imposed to the bottom, right and left boundaries of the model. The thermal and physical properties of the concrete and the soil are reported in Table 6, as indicated by Xia et al. (2012) and Sun et al. (2013). The numerical results in terms of exchanged heat per meter of pipes versus time are compared with the experimental data in Figure 3. It can be concluded that the numerical approach provides a good fit to the experimental data.

4.2. Parametric analysis

In the parametric analysis, the wall panel was considered 20 m high (D in Figure 1) and 1.5 m long (L in Figure 1), as represented in Figure 4. Accordingly, considering a depth to excavation ratio of 1.25 (lower bound of parameter 2) means an excavation of 16 m, while a ratio of 2.0 (upper bound of parameter 2) an excavation of 10 m. Within the 1.5 m length, the 25 cm pipe spacing (lower bound of parameter 3) implied the embedment of 6 pipes in a Triple-U configuration, while the 75 cm spacing (upper bound of parameter 3) resulted in 2

pipes only in a Single-U configuration (Figure 4b and c). The pipes went down to 19.5 m depth and had a diameter of 25 mm. They were positioned on the soil side of the wall only. The soil initial temperature was set equal to 12°C. The thermal and physical properties of concrete and soil are summarised in Table 7. A constant temperature, equal to the initial soil temperature, was set on the left, right and bottom boundaries of the model. The boundaries of the model were checked to be far enough not to influence the results in terms of heat exchange. Constant external air temperature was set on the excavation plane, wall side and top boundary, with a value depending on the run, i.e. equal to 14°C or 18 °C depending on the value of ΔT (Table 5). The panel width W, depth of excavation H, concrete cover C and heat-carrier fluid velocity v are also varied depending on the run as per Table 5b. The inlet temperature was imposed equal to 20°C for a simulation duration of 60 days, with an initial ramp going from 12 to 20°C lasting 5 minutes. While real systems often operate within varying and complex thermal demand (and hence inlet temperature) patterns, a constant temperature has been used to provide i) a simpler and controlled conditions comparison of the parameters under consideration and ii) a more generally applicable approach within the wide range of thermal demand scenarios relevant to different building typologies. In this case heat injection has been applied throughout. While different rates of absolute heat exchange would be obtained for heat extraction due to the temperature excess in the excavation space, only one scenario was considered, again for simplicity. This is because similar parameter rankings are to be expected from the statistical analysis regardless of the direction of heat transfer.

5. Results and discussion

The results of the eight runs are presented in Figure 5a in a semi-logarithmic plane, in terms of outlet temperature. From the difference between the inlet and outlet temperature, the exchanged power Q (measured in W) was computed as:

$$Q = m \cdot c \cdot (T_{out} - T_{in}) \quad (7)$$

where m is the mass flow rate in the pipes (measured in kg/s), c the specific heat capacity of the circulating fluid (measured in J/kg/K) and T_{out} and T_{in} the outlet and inlet fluid temperature. The resulting exchanged power per square meter of wall surface is plotted in Figure 5b.

In Figure 5b, a family of four curves (runs 2, 4, 5 and 7) showing a high initial peak can be easily distinguished. These curves result from the simulations that assume the upper bound value of fluid velocity. The initial peak is representative of the very initial phase of the simulations, during which the system is activated (imposed inlet temperature), but the heated fluid has not yet reached the outlet node. During this transient phase, the difference in temperature between the outlet and the inlet is the same for all the runs and the exchanged heat only depends on the mass flow rate in the pipes, namely on the fluid velocity (equation 7). Once the heated fluid reaches the outlet node, the amount of exchanged heat starts to be governed not only by the mass flow rate but also by the outlet temperature, which depends on the heat exchange capacity of each configuration. This occurs earlier in the simulations that consider the single-U pipe setting, explaining the different post-peak response between runs 4 & 5 and runs 2 &7.

Consequently, the high peak heat transfer rates at small simulation times are not particularly representative of longer term realistic operating conditions. By the end of the numerical simulation the heat transfer rates drop to <20 W/m^2. These values are comparable to those presented by Bourne Webb et al. (2016) and slightly lower than those suggested by Brandl (2006) as pre design values.

In the longer term, the simulations which show the highest exchange rates at 60 days are those showing the lowest temperature difference between the wall and the air in the excavation. This is more clearly shown in Figure 6, which is a zoom of Figure 5b at the long term. This is to be expected, since the simulations are injecting heat into the wall and the ground and an additional source of heat from the air inside the excavation

will be detrimental to efficiency. On the other hand, if heat was being extracted from the systems then this additional source of heat would be beneficial.

5.1. Statistical analysis

Four different time frames were considered, namely the heat transfer rate q (W/m^2) was computed at 3, 5, 30 and 60 days after the activation of the geothermal system. The obtained response table is presented in Table 8. The values contained in this table constitute the 'raw data' of the Taguchi parametric study, to which some statistical post-processing needs to be applied to extract the combination of factors (i.e. parameters) affecting the target variable (ie the heat transfer rate, q) the most. This was done interpreting the results with a level average analysis (e.g. see Peace 1993; Cecinato 2009; Cecinato & Zervos 2012). It consists of (1) calculating the average simulation result for each level of each factor, (2) quantifying the effect of each factor by taking the absolute difference between the highest and lowest average results and (3) identifying the strong effects, by ranking the factors from the largest to the smallest absolute difference. The results of the level average analyses performed for the four time frames are reported in Table 9 to Table 12, where the "Min" and "Max" values were obtained by calculating the average simulation result respectively for level 1 (low) and level 2 (high) for each factor (cf. Peace 1993, Cecinato 2009), and the "Effect" was calculated by taking the difference between "Min" and "Max" for each parameter.

Due to the statistical nature of this type of analyses, the influence of the bottom-ranked parameters cannot be assessed with confidence; hence, in the subsequent discussion attention will be principally focused on the top-five ranked parameters.

Additionally, to validate the statistical approach adopted, a so-called confirmation run (e.g. Peace 1993) was also performed. It consists of running a simulation adopting the most influential settings of the involved parameters, and comparing the result with an estimate (through statistical methods, based on positive fluctuations from the average response) of the predicted response with optimal parameter settings (in this case, parameters that maximise the heat exchange). To confirm the reliability of the statistical analysis, the outcome of the confirmation simulation q_{con} was checked to be similar to the predicted average response q_{avg}, and both values were checked to be larger than any of the responses from runs 1 to 8. As an example, after 30 days, the confirmation run resulted in q_{con}=20.6 W/m^2, with q_{ave}=18.9 W/m^2.

5.2. Discussion

As for other ground heat exchangers, the results show that the energy efficiency improves significantly if the pipe spacing is reduced, which means that increasing the number of pipes is the primary route to be considered in order to optimize the design. Indeed, spacing is among the top three parameters independently of the simulation time considered. Also increasing the concrete thermal conductivity has a positive effect, although this parameter is more difficult to engineer compared to pipe spacing. Among the three most important parameters, the other one is the temperature excess within the excavation space, which confirms in particular the benefits of exploiting the retaining walls installed for railway tunnels and metro stations. The embedment ratio, as well as concrete cover, seem to have a minor effect on the energy efficiency, as they are always ranked in the lowest positions, independently of the time frame considered. The panel width is the third most influential parameter in the short term (Table 9), but its influence decreases in the long term.

Figure 7 better illustrates the results obtained after 3, 5, 30 and 60 days of system operation, comparing the effect, as defined above, of each parameter normalized by the largest effect (i.e. the effect of the most influential parameter) in the same time frame. The rankings of each parameter for each time frame are also reported for completeness. Interesting observations can be drawn regarding the trends of the parameters' influence with time, distinguishing those that play a major role in the short or in the long term.

In the very short term, the four most influential parameters are pipe spacing, concrete conductivity, panel width and fluid velocity. However, as the heat exchange process proceeds from the initial transient condition towards a steady state condition, the difference in temperature between the air inside the excavation and the soil becomes the predominant factor, to the detriment mainly of the panel width. This is consistent with the long term steady state analysis carried out by Bourne Webb et al. (2016) which showed heat transfer to be dominated by the interface with the inside of the excavation. The effect of pipe spacing correspondingly decreases as time progresses, but always remains among the top three parameters. Given the importance of both the temperature excess between the wall and the excavation and the pipe spacing the results of this new analysis suggests that equipping both sides of the wall with pipes over its full depth would therefore be beneficial for energy efficiency. The results of the analysis with respect to pipe spacing can be also compared with the analysis carried out by ICConsulten (2005) which suggested an optimal pipe spacing of between 40 cm and 60 cm when also considering long term pay back periods and a balance between heating and cooling applications.

The third important parameter identified in Figure 7 is concrete conductivity. Its ranking varies but it always remains in the top three. This suggest that where possible seeking to actively engineer the concrete mix for thermal effectiveness would be beneficial. Measures could include using high silica content aggregate and minimising the use of admixtures. None of panel width, concrete cover or fluid velocity are consistently important parameters in the analysis. The latter is in accordance with other studies on energy piles (Cecinato & Loveridge 2015; Loveridge & Cecinato 2016; Sterpi et al. 2014). Finally, the ratio of the excavation depth to the wall depth is also seen to be of limited importance. This result was not expected given the effect the excavation air temperature is seen to have on the energy exchanged. However, it is possible that this could be more important at steady state which was not considered in this set of simulations.

6. Conclusions and Recommendations

The possibility of coupling the structural function of diaphragm walls with their exploitation as ground heat exchangers has been explored in recent years resulting in a number of successfully implemented case studies. However, there has remained a lack of systematic analysis to consider the parameters which govern the energy efficiency of this technology. Using numerical simulation and statistical analysis this study has shown that:

1. For short term considerations the pipe spacing is the most important factor affecting energy efficiency and this suggests that maximising the number of pipes installed is one route to optimisation. However, it is also observed that the pipe spacing influence reduces with time and hence other factors including long term payback periods need to be considered for finalising of design spacings.
2. In the long term the temperature excess between the wall and the excavation is the single most important factor governing energy efficiency. This illustrates the point that “hot excavations” like metro stations and shallow rail tunnels are particularly well suited for energy extraction, but poorly suited for waste heat disposal. To take advantage of this additional renewable heat source then it is suggested that the pipes be installed on both sides of the diaphragm wall in addition to optimisation of spacing as indicated above.
3. The thermal properties of the concrete forming the wall are also of importance in energy efficiency. Consequently, where possible it is recommended to engineer the concrete mix for maximum thermal conductivity through use of silica rich aggregates and reduced application of admixtures.

This study represents a first high level study on an efficiency framework for diaphragm walls used for heat exchange. Further work is required to consider other aspects in more detail, for example the effect of a convective boundary condition inside a shallow tunnel should be accurately investigated. More detailed analysis assessing the added efficiency of equipping both sides of the energy wall as a ground heat exchanger would also be beneficial.

Acknowledgements

This work was carried out in the framework of the COST Action GABI TU 1405, European network for shallow geothermal energy applications in buildings and infrastructures. Fleur Loveridge is funded by the Royal Academy of Engineering under their Research Fellow scheme.

7. References

Amis, T., Robinson, C. & Wong, S., 2010. Integrating Geothermal Loops into the Diaphragm Walls of the Knightsbridge Palace Hotel Project, geotechnical challenges in urban regeneration. *Proceeding of the 11th DFI / EFFC International conference, London*, p.10.

Ampofo, F., G, M.G. & Missenden, J.F., 2011. Application of groundwater cooling scheme for London Underground Network. *International Journal of Refridgeration*, 34(8), pp.2042–2049.

Ampofo, F., Maidment, G. & Missenden, J., 2004. Underground railway environment in the UK Part 2 : Investigation of heat load. *Applied Thermal Engineering*, 24, pp.633–645.

Barla, M., Di Donna, A. & Perino, A., 2016. Application of energy tunnels to an urban environment. *Geothermics*, 61, pp.104–113.

Barla, M. & Perino, A., 2015. Energy from geo-structures: a topic of growing interest. *Environmental Geotechnics*, 2(1), pp.3–7.

Batini, N. et al., 2015. Energy and geotechnical behaviour of energy piles for different design solutions. *Applied Thermal Engineering*, 86, pp.199–213.

Bourne-Webb, P.J., Bodas Freitas, T.M. & da Costa Gonçalves, R.A., 2016. Thermal and mechanical aspects of the response of embedded retaining walls used as shallow geothermal heat exchangers. *Energy and Buildings*, (doi: 10.1016/j.enbuild.2016.04.075).

Bourne-Webb, P.J., da Costa Goncalves, R.A. & Bodas Freitas, T.M., 2015. Retaining walls as heat exchangers: a numerical study. In *Proceedings of the XVI ECSMGE Geotechnical Engineering for Infrastructure and Development*. (doi: 10.1680/ecsmge.60678), pp. 2499–2504.

Brandl, H. et al., 2010. Concrete absorber technology for earth coupled concrete structures using geothermal energy for the Vienna Undeground line U2. *Ingenieur und Architekten Zeitschrift*, 155(Heft 7-9/2010 & Heft 10-12/2010).

Brandl, H., 2006. Energy foundations and other thermo-active ground structures. *Géotechnique*, 56(2), pp.81–122.

Brandl, H., 1998. Energy piles and diaphragm walls for heat transfer from and into ground. In *3rd International Symposium on Deep Foundations on Bored and Auger Piles (BAP III)*. pp. 37–60.

BS EN ISO 6946:2007, 2007. *Building components and building elements. Thermal resistance and thermal transmittance. Calculation method.*, ISBN: 978 0 580 54937 3.

Burland, J. et al., 2012. *ICE Manual of Geotechnical Engineering* L. Thomas Telford, ed., London.

Cecinato, F. et al., 2015. A new modelling approach for piled and other ground heat exchanger applications. In *Proc. XVI ECSMGE 2015*. Edimburgh, UK.

Cecinato, F., 2009. *The role of frictional heating in the development of catastrophic landslides.* PhD thesis, University of Southampton.

Cecinato, F. & Loveridge, F., 2015. Influences on the thermal efficiency of energy piles. *Energy*, 82, pp.1021–

1033.

Cecinato, F. & Zervos, A., 2012. Influence of thermomechanics in the catastrophic collapse of planar landslides. *Canadian Geotechnical Journal*, 49, pp.207–225.

Diersch, H.J.G., 2009. DHI Wasy Software - Feflow 6.1 - Finite Element Subsurface Flow & Transport Simulation System: Reference Manual.

Di Donna, A., 2016. Energy walls for an underground car park. In *25th European Young Geotechnical Engineering conference*. 21-24 June 2016, Sibiu, Romania.

Di Donna, A. & Barla, M., 2015. The role of ground conditions and properties on the efficiency of energy tunnels. *Environmental geotechnics*, (doi: 10.1680/jenge.15.00030), pp.1–11.

Duris, L., Aldorf, J. & Geryk, J., 2013. Thermal loading action on final linings of underground structures. *Tunnel*, 22(2), pp.44–52.

Gaba, A.R. et al., 2003. *Embedded retaining walls – guidance for economic design*, CIRIA C580, Construction Industry Research and Inf.

ICConsulten, 2005. *Wirtschaftliche optimierung von tunnelthermieabsorberanlagen, grundlagenuntersuchung und planungsleitfaden*, 23.12.2005. Rev 1, 84 pp.

Kurten, S., 2014. *Zur thermischen Nutzung des Untergrunds mit flächigenthermo-aktiven Bauteilen*. PhD thesis, Aachen University.

Kurten, S., Mottaghy, D. & Ziegler, M., 2015. Design of plane energy geostructures based on laboratory test and numerical modelling. *Energy and Buildings*, 107, pp.434–444.

Loveridge, F. & Cecinato, F., 2016. Thermal performance of thermoactive continuous flight auger piles. *Environmental geotechnics*, (10.1680/jenge.15.00023).

Markiewicz, R., 2004. *Numerical and experimental investigations for utilization of geothermal energy using earth-coupled structures and new developments for tunnels*. PhD thesis, Vienna University of Technology.

Nicholson, D. et al., 2014. The design of thermal tunnel energy segments for Crossrail, UK. *Proceedings of the Institution of Civil Engineers - Engineering Sustainability*, 167(ES3), pp.118–134.

Ordody, P., 2000. Thermal Comfort in the Passenger Areas of the Budapest Metro. *Periodica Polytechnica Ser Mech Eng*, 44(2), pp.309–317.

Peace, G.S., 1993. *Taguchi methods: a hands-on approach* M. Addison-Wesley, Reading, ed.,

Rui, Y., 2014. *Finite Element Modelling of Thermal Piles and Walls*. PhD thesis, University of Cambridge.

Soga, K., Qi, H., Rui, Y. & Nicholson, D., 2014. Some considerations for designing GSHP coupled geotechnical structures based on a case study. In *7th International Congress onEnvironmental Geotechnics*. Melbourne, Australia.

Sterpi, D. et al., 2014. Numerical analysis of heat transfer in thermo-active diaphragm walls. *Numerical methods in geotechnical engineering*, pp.1043–1048.

Sun, M., Xia, C. & Zhang, G., 2013. Heat transfer model and design method for geothermal heat exchange tubes in diaphragm walls. *Energy and Buildings*, 61, pp.250–259.

Taguchi, G., El Sayed, M. & Hsaing, C., 1989. *Quality engineering and quality systems* N. Y. McGraw-Hill, ed., New York.

Xia, C. et al., 2012. Experimental study on geothermal heat exchangers buried in diaphragm walls. *Energy and*

Buildings, 52, pp.50–55.

Zhang, G. et al., 2013. A new model and analytical solution for the heat conduction of tunnel lining ground heat exchangers. *Cold Regions Science and Technology*, 88, pp.59–66.

Table 1 - Geometric Information from Constructed Energy Diaphragm Walls

Case & References	Wall Depth D	Embedment Depth[1] D-H	Panel Width W	Panel Length L	Pipes spacing (Ground Side) sp	Pipes on Excavation Side?	Pipe cover C	Pipe Size (O.D.)
U2 Taborstrasse Station, Vienna (Brandl et al. 2010; Markiewicz 2004)	31m	10.45m	0.8m		0.53m	Yes	60mm (to steel, pipes inside steel)	25mm
Shanghai Museum of Nature History (Xia et al. 2012; Sun et al. 2013)	30 – 38m	12m – 20m	1.0m	3.7m	1 U-loop per panel	Yes	87.5mm	25mm
Bulgari Hotel (formerly Knightsbridge Palace Hotel) (Amis et al. 2010)	Up to 36m	11.65m	0.8m		0.84 (average)	No	75mm	
Dean Street Station, London (Rui 2014)	41m	12m	1.0m					
Tottenham Court Road Station, London			1.2m	3m	0.5m	No	40mm (pipes in 75mm cover zone)	35mm
Moorgate Shaft, London	48.5m to 52.4m		1.2m		0.5m (average)	No	62.5mm	25mm
Arts Centre, Bregenz, Austria (Brandl 1998)	Up to 28m	Up to 17m	0.5m to 1.2m		A wavy or slinky type arrangement was used			

[1] Including any slab thickness

Table 2 - Heat Transfer Coefficients Adopted in Energy Geostructure Analysis.

Case & Source	Scenario	Heat Transfer Coefficient, h (W/m^2K)	Comments
Lainzer Tunnel, Austria. Sensitivity analysis (ICConsulten 2005)	Metro tunnels & stations	10 - 15	
Generic Case. General sensitivity analysis only (Bourne-Webb et al. 2016; Bourne-Webb et al. 2015)	Not specified	2.5 - 25	Depending on wind speed
Mongolian Road Tunnel. Field study and analytical model (Zhang et al. 2013; Nicholson et al. 2014);	Road tunnel	15	Not diaphragm wall, but comparable analysis
Bored Tunnel, London. Analysis only (Nicholson et al. 2014)	Rail tunnel	5	Not diaphragm wall, but comparable analysis
Laboratory experiment. Analytical and numerical studies (Kurten 2014)	Basements	7.7	Based on ISO 6946

Table 3 – Tunnel air temperatures.

Case & Source	Scenario	Annual temperature (°C)	Comments
Section LT24 Lainzer tunnel (Brandl 1998)	Metro tunnels & stations	5 to 15	In line with seasonal changes
U2 Vienna Metro line (Brandl 1998)	Metro tunnel	10 to 20	Equal to outside air temperature in summer, up to 20 °C higher than outside temperature in winter
Tunnel in Czech Republic (Duris et al. 2013)	Road tunnel	18 to 28 (summer) and -5 to -15 (winter)	In phase with outside temperature
Budapest Metro (Ordody 2000)	Deep metro	15 to 20	Small lag compared with outside air temperature
Victoria Line, London Underground (Ampofo et al. 2011)	Deep metro	22 - 31	Summer platform air temperature
Torino metro tunnel (Barla & Perino 2015; Barla et al. 2016)	Metro tunnel	12 - 27	In line with seasonal changes

Table 4 - Parameters investigated in the parametric analysis.

Parameter number	Parameters	Lower value	Upper value
1	Panel width, W (m)	0.8	1.2
2	Depth/excavation ratio, R (-)	1.25	2.0
3	Spacing of pipes, sp (cm)	25	75
4	Concrete cover to pipes, C (mm)	50	100
5	Fluid velocity, v (m/s)	0.2	1.2
6	Difference between soil and excavation air temperature, ΔT (°C)	2	6
7	Concrete conductivity, λ_{conc} (W/mK)	1.5	3.0

Table 5 – Taguchi "L8" seven parameter set: (a) standard array and (b) application to the specific case study.

		Parameter number						
		1	**2**	**3**	**4**	**5**	**6**	**7**
Run number	**1**	1	1	1	1	1	1	1
	2	1	1	1	2	2	2	2
	3	1	2	2	1	1	2	2
	4	1	2	2	2	2	1	1
	5	2	1	2	1	2	1	2
	6	2	1	2	2	1	2	1
	7	2	2	1	1	2	2	1
	8	2	2	1	2	1	1	2

(a)

		Parameter						
		W [m]	**R [-]**	**sp [cm]**	**C [mm]**	**v [m/s]**	**ΔT [°C]**	**λ_{conc} [W/m/K]**
Run number	**1**	0.8	1.25	25	50	0.2	2.0	1.5
	2	0.8	1.25	25	100	1.2	6.0	3.0
	3	0.8	2.0	75	50	0.2	6.0	3.0
	4	0.8	2.0	75	100	1.2	2.0	1.5
	5	1.2	1.25	75	50	1.2	2.0	3.0
	6	1.2	1.25	75	100	0.2	6.0	1.5
	7	1.2	2.0	25	50	1.2	6.0	1.5
	8	1.2	2.0	25	100	0.2	2.0	3.0

(b)

Table 6 - Properties of the materials involved in the validation analysis (Xia et al., 2012 and Sun et al., 2013).

Property	Concrete	Soil	Heat carrier fluid
Bulk thermal conductivity, λ [W/m/K]	2.34	1.74	0.58
Bulk specific heat capacity, c [J/kg/K]	1046	1690	4200
Bulk density, ρ [kg/m^3]	2500	1800	1000
Porosity, n [-]	0	0.25	-
Specific storage, S [1/m]	10^{-4}	10^{-4}	-
Hydraulic conductivity, K_{ij} [m/s]	0	10^{-4}	-
Longitudinal dispersivity, α_L [m]	5	5	-
Transversal dispersivity, α_T [m]	0.5	0.5	-

Table 7 - Thermal properties of the materials in the parametric analyses.

Property	Concrete	Soil	Heat carrier fluid
Bulk thermal conductivity, λ (W/m/K)	Depends on the run	2.0	0.6
Bulk specific heat capacity, c (J/kg/K)	1600	1600	4200
Bulk density, ρ (kg/m^3)	2210	1900	1000
Porosity, n (-)	0	0.3	-
Specific storage, S [1/m]	10^{-4}	10^{-4}	-
Hydraulic conductivity, K_{ij} [m/s]	0	10^{-4}	-
Longitudinal dispersivity, α_L [m]	5	5	-
Transversal dispersivity, α_T [m]	0.5	0.5	-

Table 8 - Response table

Factors									Results			
		W [m]	R [-]	sp [cm]	C [mm]	v [m/s]	ΔT [°C]	λ_c [W/m/K]	q - 3 days (W/m^2)	q - 5 days (W/m^2)	q - 30 days (W/m^2)	q - 60 days (W/m^2)
Run number	1	0.8	1.25	25	50	0.2	2	1.5	30.8	24.6	15.1	13.3
	2	0.8	1.25	25	100	1.2	6	3	33.5	24.8	13.9	11.8
	3	0.8	2	75	50	0.2	6	3	23.2	19.0	9.8	7.7
	4	0.8	2	75	100	1.2	2	1.5	22.0	19.3	11.7	9.8
	5	1.2	1.25	75	50	1.2	2	3	31.8	26.8	15.7	14.0
	6	1.2	1.25	75	100	0.2	6	1.5	18.8	15.9	7.2	5.5
	7	1.2	2	25	50	1.2	6	1.5	37.2	27.6	10.9	8.1
	8	1.2	2	25	100	0.2	2	3	38.8	30.7	16.8	18.4

Table 9 - Results of level average analysis after 3 days.

	W [m]	R [-]	Sp [cm]	C [mm]	v [m/s]	ΔT [°C]	λ_c [W/m/K]
Min	27.41	28.75	35.09	30.75	27.93	30.87	27.22
Max	31.65	30.31	23.97	28.31	31.13	28.19	31.84
Effect	4.23	1.56	11.12	2.45	3.20	2.68	4.62
Ranking	**3**	**7**	**1**	**6**	**4**	**5**	**2**

Table 10 - Results of level average analysis after 5 days.

	W [m]	R [-]	Sp [cm]	C [mm]	v [m/s]	ΔT [°C]	λ_c [W/m/K]
Min	21.94	23.04	26.94	24.52	22.58	25.36	21.85
Max	25.25	24.16	20.26	22.68	24.62	21.84	25.35
Effect	3.31	1.11	6.68	1.83	2.05	3.52	3.50
Ranking	**4**	**7**	**1**	**6**	**5**	**2**	**3**

Table 11 - Results of level average analysis after 30 days.

	W [m]	R [-]	Sp [cm]	C [mm]	v [m/s]	ΔT [°C]	λ_c [W/m/K]
Min	12.63	12.97	14.17	12.86	12.21	14.81	11.21
Max	12.64	12.30	11.10	12.41	13.06	10.46	14.05
Effect	0.01	0.67	3.07	0.46	0.85	4.35	2.84
Ranking	**7**	**5**	**2**	**6**	**4**	**1**	**3**

Table 12 - Results of level average analysis after 60 days.

	W [m]	R [-]	Sp [cm]	C [mm]	v [m/s]	ΔT [°C]	λ_c [W/m/K]
Min	10.65	11.14	12.91	10.77	11.22	13.88	9.19
Max	11.49	11.01	9.24	11.37	10.93	8.26	12.96
Effect	0.84	0.14	3.68	0.60	0.29	5.62	3.77
Ranking	**4**	**7**	**3**	**5**	**6**	**1**	**2**

Figure 1 - Geometry parameters.

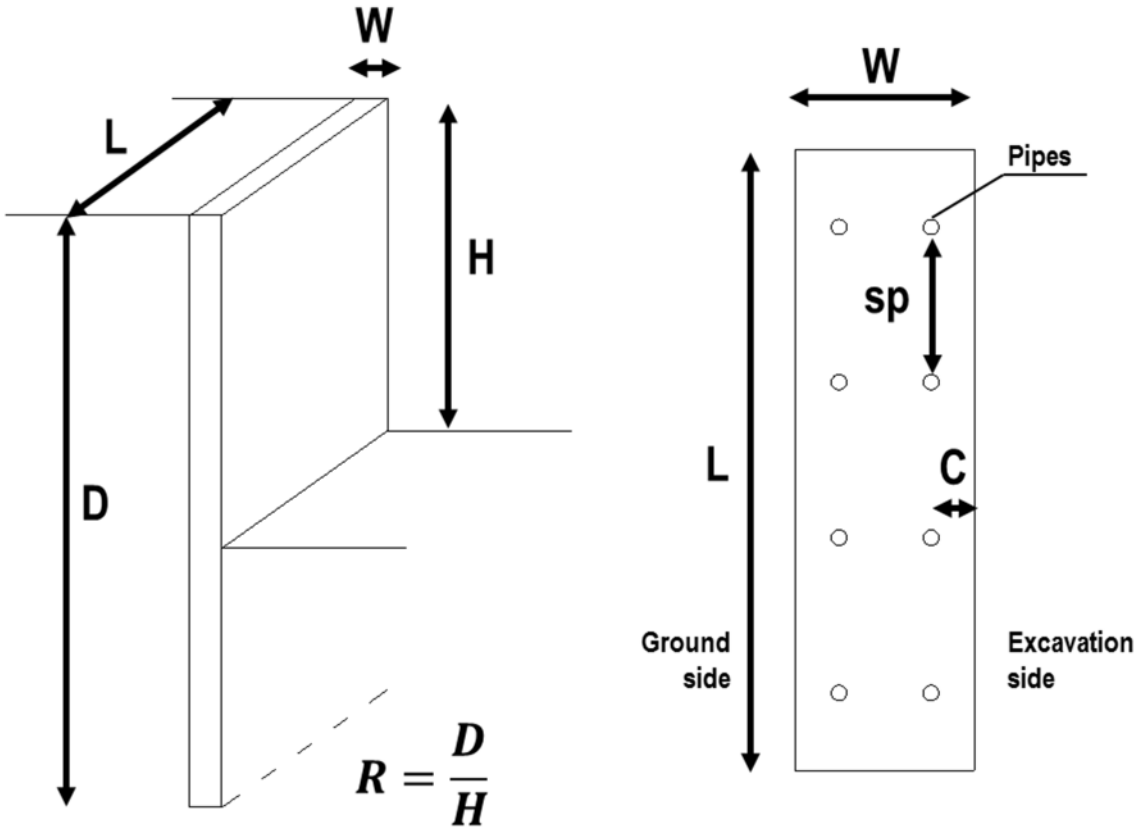

Figure 2 – (a) Geometry of the wall (soil neglected for clarity) and (b) FE model of the validation test.

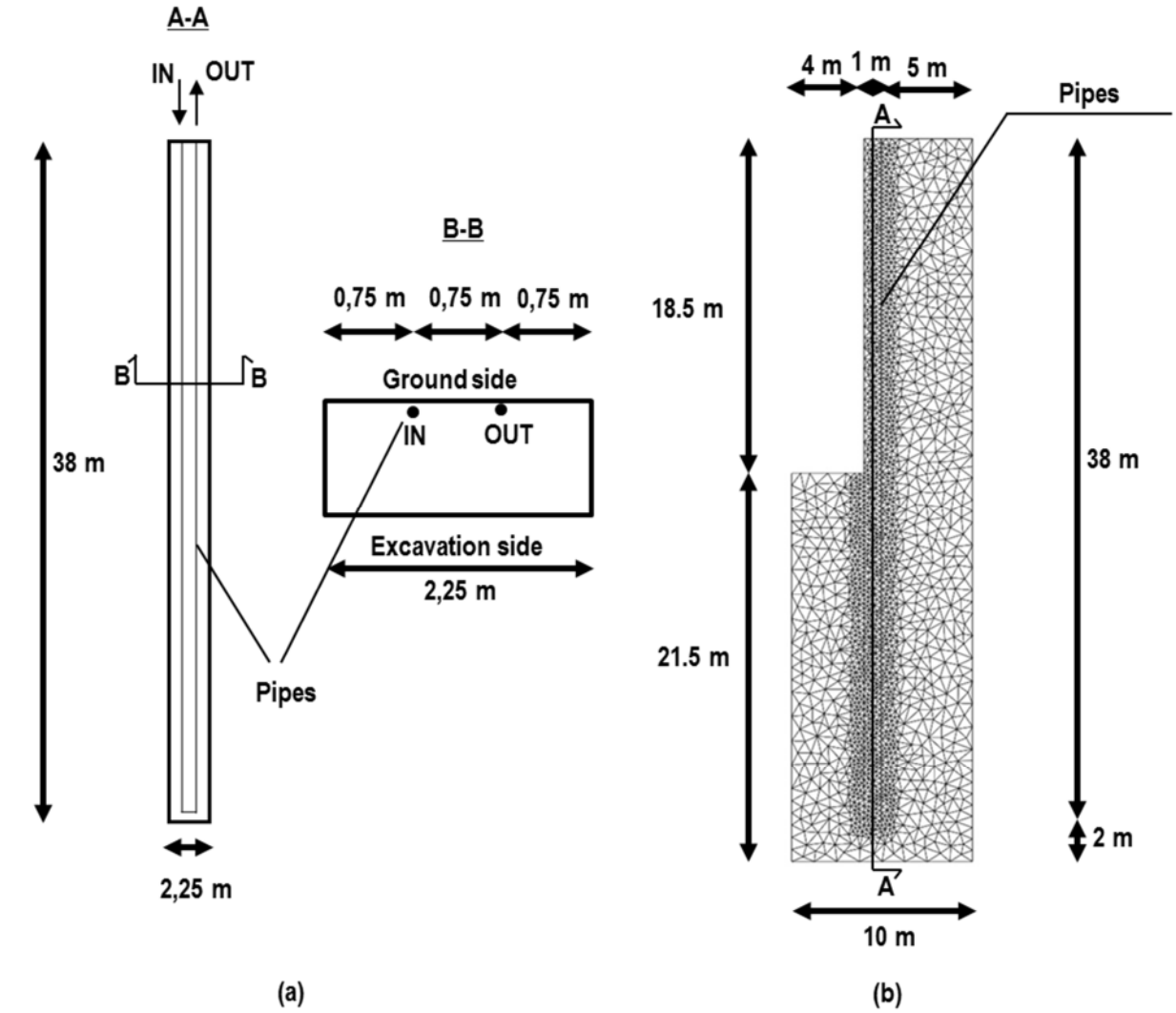

Figure 3 - Validation of the numerical approach (experimental data from Xia et al. (2012)) showing heat transfer per unit pipe length against time.

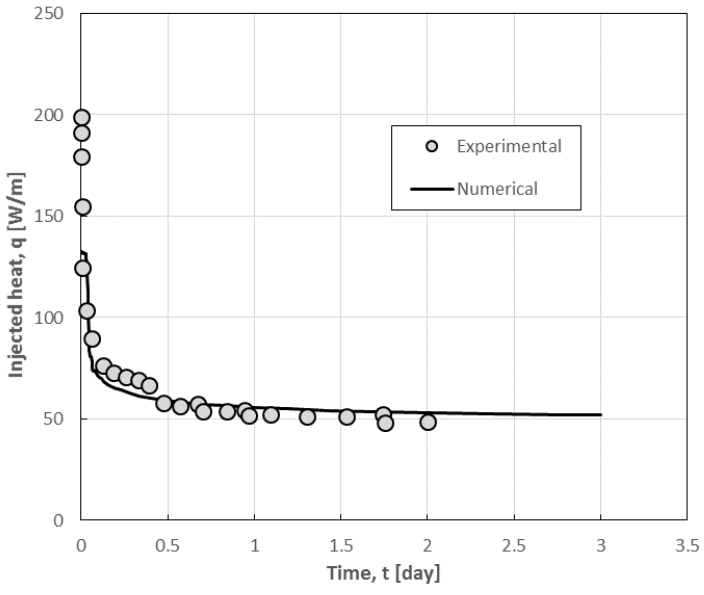

Figure 4 – Problem geometry for the parametric analysis: (a) vertical cut of the FE model, (b) vertical cut and (c) horizontal cut of the wall panel assuming upper and lower values of pipe spacing.

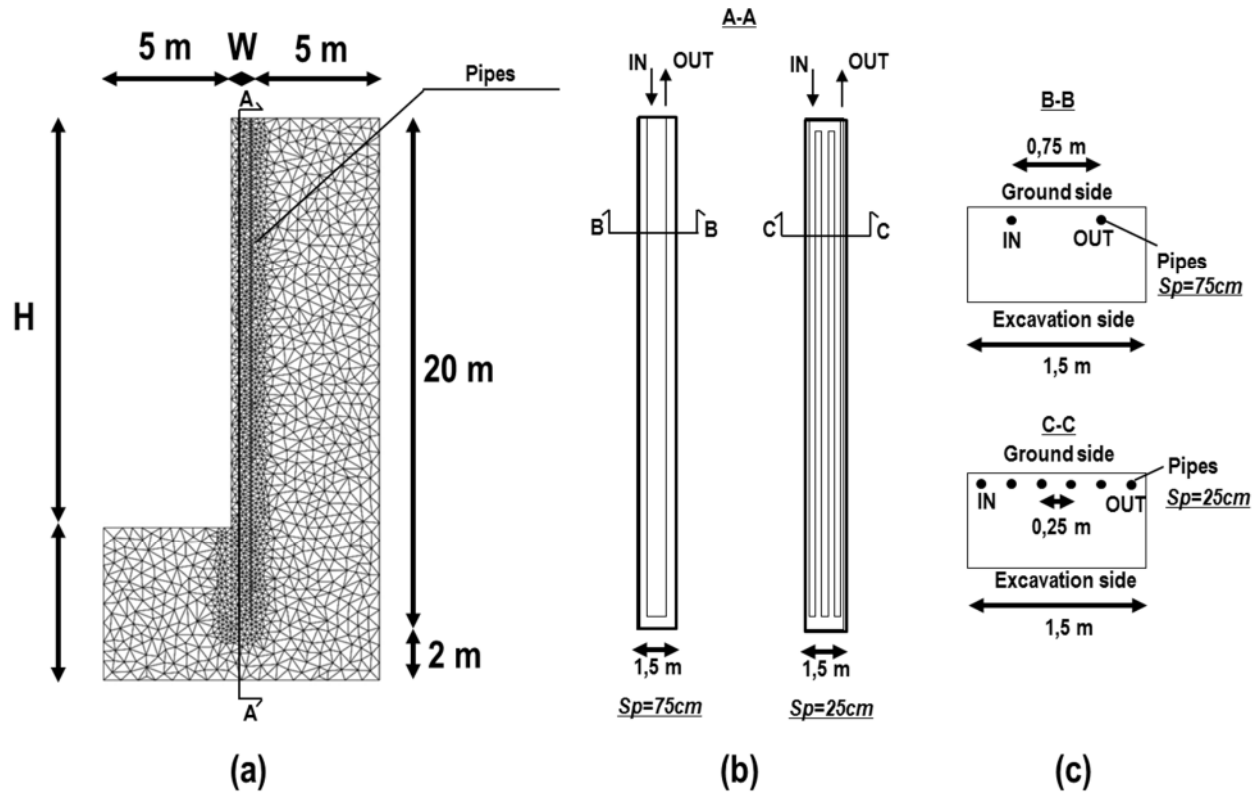

Figure 5 - Results of the parametric analysis: (a) outlet temperature and (b) exchanged power per square meter of wall surface.

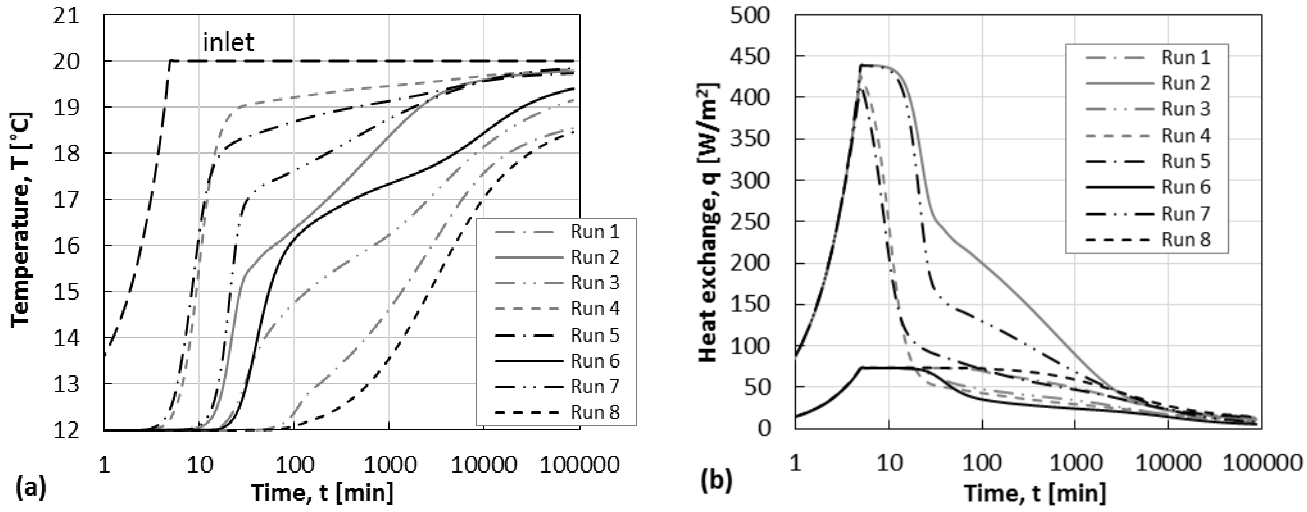

Figure 6 – Exchanged power per square meter of wall surface in the long term.

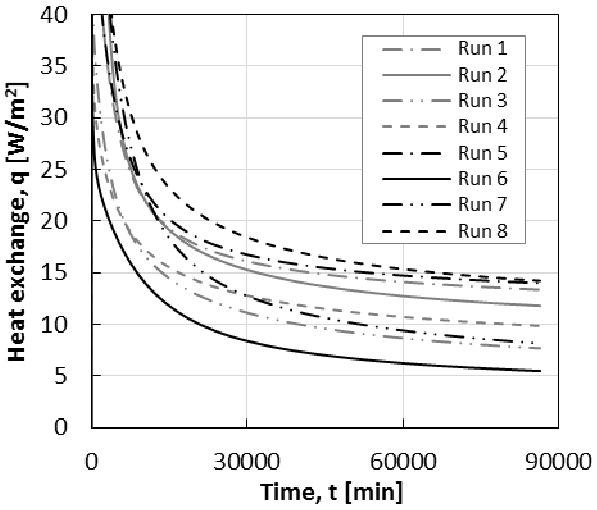

Figure 7 – Normalised effect of each parameter in terms of heat exchanged.